Carbohydrate Polymers 102 (2014) 453–459

Contents lists available at ScienceDirect

Carbohydrate Polymers

journal homepage: www.elsevier.com/locate/carbpol

Effects of amylose content on property and microstructure of starch-graft-sodium acrylate copolymers

Zhi Zhang[a,c], Peirong Chen[a,*], Xianfeng Du[b,**], Zhonghua Xue[a,c], Shanshan Chen[a], Baojun Yang[c]

[a] Department of Applied Chemistry, School of Science, Anhui Agricultural University, Hefei 230036, China
[b] School of Tea & Food Science and Technology, Anhui Agricultural University, Hefei 230036, China
[c] Department of Chemical Processes, School of Chemical Engineering, Hefei University of Technology, Hefei 230009, China

ARTICLE INFO

Article history:
Received 2 August 2013
Received in revised form
20 November 2013
Accepted 21 November 2013
Available online 2 December 2013

Keywords:
Superabsorbent copolymer
Starch
Microstructure
Amylose
Graft

ABSTRACT

Starch-graft-sodium acrylate (St-g-SA) copolymers were synthesized with ammonium persulfate as an initiator. This work focused on the effects of amylose content of corn starch on the water absorbent capacity and microstructure of the St-g-SA copolymers. The water absorbent capacity of waxy, maize and high amylose St-g-SA copolymers was 1800 g/g, 1300 g/g and 1100 g/g respectively. The grafted copolymers were characterized by FTIR and solid state ^{13}C NMR confirming that the graft reaction had taken place between sodium acrylate and corn starch. The surfaces and cross sections of St-g-SA copolymers were observed by SEM. Incomplete gelatinized starch aggregates increased with increasing amylose content on surfaces and cross sections of copolymers, which accorded with the water absorbent capacity and grafting ratio. DMTA results showed that the waxy St-g-SA copolymer had the highest transition temperature which indicated waxy starch had high grafting ratio.

1. Introduction

Superabsorbent polymers are three-dimensional networks, which are composed of homopolymers or copolymers and are insoluble in all solvents. Depending on their compatibility with the solvent, they can absorb and hold a considerable volume of liquids (Athawale & Lele, 2001; Hua & Wang, 2008; Jiraprasertkul, Nuisin, Jinsart, & Kiatkamjornwong, 2006). Owing to their excellent properties of superabsorbent, superabsorbent polymers are widely used in many fields, such as flocculants for wastewater treatment (Güçlü, Güçlü, & Keleş, 2007; Güçlü et al., 2010; Jiraprasertkul et al., 2006), drug delivery systems (Ameye et al., 2001; Coucke et al., 2009), biological (Ameye et al., 2002; Eid, 2008) and hygienic products, particularly disposable diapers and napkins, in which they are used to capture secreted fluids such as urine and blood (Zou et al., 2012). St-g-SA copolymer is one of superabsorbents having a greater demand in industry due to their low cost and also because of the certain proportion of starch in these polymers which render them biodegradable and environmental friendly.

Previous reports show that properties of corn starch are different with different amylose content (Matveev et al., 2001). Furthermore, it is shown that the native granule structure, the melting thermodynamic parameters and the functional properties of starches are influenced by the amylose content (Kiseleva et al., 2005; Sang, Bean, Seib, Pedersen, & Shi, 2008). Amylose content of starches on physical properties and biodegradability of starch/PVA-blended films also exhibits a strong influence (Yun & Yoon, 2010). In addition, starch-based superabsorbent polymers grafting ratio, grafting efficiency, graft position and length of the grafted segment have recently been investigated for explaining graft reaction and performance of starch-based superabsorbents with different amylose/amylopectin ratio in starches (Zou et al., 2012). Application of starch always involves gelatinization of starch that breaks the interchains hydrogen bonding so as the rheological properties of starch paste can be utilized effectively and that induces a complex structural modification, leading to dramatic apparent viscosity change. Besides temperature, gelatinization behaviors of corn starches with different amylose content are also obviously different (Liu, Yu, Xie, & Chen, 2006).

St-g-SA copolymers are used extensively as superabsorbents, which show high swelling capacity. It is important to have a relatively complete cognition to internal structure of superabsorbent polymeric network because high water absorbent capacity needs high cooperative among composites that is the reflection to

* Corresponding author. Tel.: +86 551 65786121; fax: +86 551 65786121.
** Corresponding author. Tel.: +86 551 65786405; fax: +86 551 65786405.
E-mail addresses: chenpeirong@ahau.edu.cn (P. Chen), dxf@ahau.edu.cn (X. Du).

0144-8617/$ – see front matter © 2013 Published by Elsevier Ltd.
http://dx.doi.org/10.1016/j.carbpol.2013.11.027

internal stimuli such as osmotic pressure, amylose content of starch, et al. Therefore, it is significant and urgent to research the effect of amylose content on internal microstructure and graft ratio of St-g-SA copolymers, which is closely connected to water absorbent capacity. Corn starches with different amylose contents (waxy, 5%; maize, 27%; high amylose, 70%) were used as model materials to synthesize the superabsorbent graft copolymer using ammonium persulfate as an initiator and N,N′-methylene-bisacrylamide as a crosslinker.

2. Materials and methods

2.1. Materials

Corn starches with different amylose contents according to the manufacturer were used in the experimental work as model materials. High amylose starch (70% amylose content) was supplied by National Starch, America. Maize starch (27% amylose content) was supplied by Shandong Jincheng Co., Ltd., China. Waxy starch (5% amylose content) was supplied by Shandong Jincheng Co., Ltd., China. All other chemicals used in the work were also commercially available. Ammonium persulfate was obtained from Shantou West Long Chemical Co., Ltd. N,N′-methylene-bisacrylamide was from Sinopharm Chemical Reagent Co., Ltd. Acrylic acid (AA) was from Tianjin Guangfu Fine Chemical Research Institute. Sodium hydroxide was from Shantou West Long Chemical Co., Ltd.

2.2. Preparation of copolymers

A 250 mL four-neck round-bottom flask equipped with a mechanical stirrer (Gongyi SZCL-3A, two blade propeller type, 400 rpm) and a nitrogen line was charged with 120 mL of water and 5.00 g of waxy or maize starch and the mixture was stirred for 30 min at 100 °C, while the high amylose starch was heated and stirred in an autoclave for 30 min at 120 °C. The gelatinized starch was subsequently cooled to room temperature. Then after adding ammonium persulfate (0.16 g) and N,N′-methylene-bisacrylamide (0.012 g), 95% neutralized acrylic acid (20.00 g) regarded as monomer was added to the flask. The mixture was heated in thermostatic water bath at 65 °C for 5 h under nitrogen atmosphere to obtain hydrogel, as reported previously (Cao, Xu, Feng, & Wang, 2005; Hua & Wang, 2008; Wu, Wei, Lin, & Lin, 2003). Poly (sodium acrylate) (PSA) hydrogel was synthesized under the same conditions with no added starch. These obtained hydrogels were further processed.

A portion of hydrogels were washed with distilled water and rewashed with ethanol to remove ungrafted molecules and acrylic acid homopolymer to achieve the grafted copolymers (Jyothi & Carvalho, 2013; Lanthong, Nuisin, & Kiatkamjornwong, 2006; Wu, 2005; Zhang, Wang, & Wang, 2007; Zou et al., 2012). The grafted copolymers were dried at 105 °C, crushed and sieved through a 200-mesh (75 μm-mesh) screen to obtain powders for FTIR analysis and grafting ratio calculation, respectively. Another portion of hydrogels were washed thoroughly by acetone to remove unreacted acrylic acid and homopolymer until the precipitate agglomerates. Both the grafted copolymer and maybe ungrafted starch were separated by centrifugation. The precipitate was dried in a vacuum oven at 60 °C until constant weight. The dried samples were crushed and sieved through a 200-mesh screen to obtain powders for the ^{13}C NMR analysis (Witono, Marsman, Noordergraaf, Heeres, & Janssen, 2013). The remainder hydrogels were poured onto a polytetrafluoroethylene dish and were dried at 65 °C to solid state, then dried at 105 °C to a constant weight to form the films for characterizations of the water absorbent capacity, SEM, DMTA and mechanical properties.

2.3. Characterizations

2.3.1. Fourier transforms infrared spectrometer (FTIR)

The starches, grafted copolymers and PSA were characterized by Nicolet-Nexus 670 model FTIR spectrophotometer using KBr pellets.

2.3.2. Solid state ^{13}C NMR spectroscopy

Solid state ^{13}C NMR spectra were recorded on Bruker AV400 spectrometer operating at 100.62 MHz. The powders of starch, copolymers, and PSA were packed into 4 mm rotors and spun at speeds of 5 kHz and a fixed CP contact time of 2 ms was used in all the experiments.

2.3.3. Water absorbent capacity of copolymers

The water absorbent capacity of copolymer was measured by a filtration method. St-g-SA copolymers films were bended to break into small pieces, 0.10 g of several pieces of dry film was put into distilled water, and completely immersed in excess water for 24 h to reach swelling equilibrium at ambient temperature (Lanthong et al., 2006; Wu et al., 2003). The fully swollen copolymer gels were filtered through a 100-mesh (150 μm-mesh) nylon screen to remove the residual water. The absorption capacity Q (g/g) was calculated as shown in Eq. (1) (Cao et al., 2005; Lanthong et al., 2006; Zhang et al., 2007).

$$Q = \frac{M_2 - M_1}{M_1} \quad (1)$$

where M_1 (g) is the weight of the dry film sample, M_2 (g) is the weight of the swollen gel sample.

2.3.4. Grafting ratio

In a 125 mL Erlenmeyer flask mounted with a condenser, 0.5 g of the grafted copolymer was refluxed in 50 mL of 1 M HCl at 100 °C for 2 h (Lanthong et al., 2006). The polymer was filtered and washed with distilled water to a pH of 7, and then it was dried at 105 °C to obtain grafted polymer. Iodine solution was applied to observe the completion of acid hydrolysis starch reaction. The grafting ratio (GR) was calculated by Eq. (2) (Jyothi & Carvalho, 2013; Lanthong et al., 2006; Zhu, Li, & Jin, 2009; Zou et al., 2012).

$$GR(\%) = \frac{W_1}{W_o} \times 100\% \quad (2)$$

where W_1 (g) is the weight of grafted polymer and W_o (g) is the weight of starch.

2.3.5. Field emission scanning electron microscope (SEM)

The morphology observation was carried out by Sirion200 Scanning Electron Microscopy (SEM). Firstly, St-g-SA copolymers films obtained by drying the synthesized hydrogels were directly bended to break into pieces, then these pieces of dry film were coated with gold. Finally, the film upper surface contacted with the air during drying process and the film broken cross section were observed to take images for surface and cross section, respectively.

2.3.6. Dynamic mechanical thermal analysis (DMTA)

St-g-SA copolymers and PSA films (30 mm × 5 mm × 1 mm) were performed on DMA 242E (Netzsch) analyzer at a frequency of 1 Hz and a displacement of ±60 mm (about 0.1 N in force), from room temperature to 180 °C at a heating rate of 5 °C/min under nitrogen atmosphere (100 mL/min), using the single cantilever bending mode.

2.3.7. Mechanical properties of copolymers

Elongation at break and tensile strength were evaluated for St-g-SA copolymers and PSA films (50 mm × 5 mm × 1 mm) using the

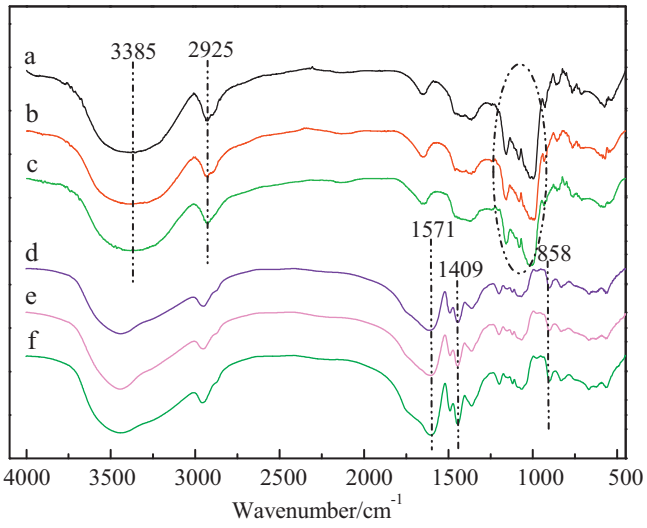

Fig. 1. FTIR spectra of (a) waxy starch, (b) maize starch, (c) high amylose starch, (d) waxy St-g-SA copolymer, (e) maize St-g-SA copolymer and (f) high amylose St-g-SA copolymer.

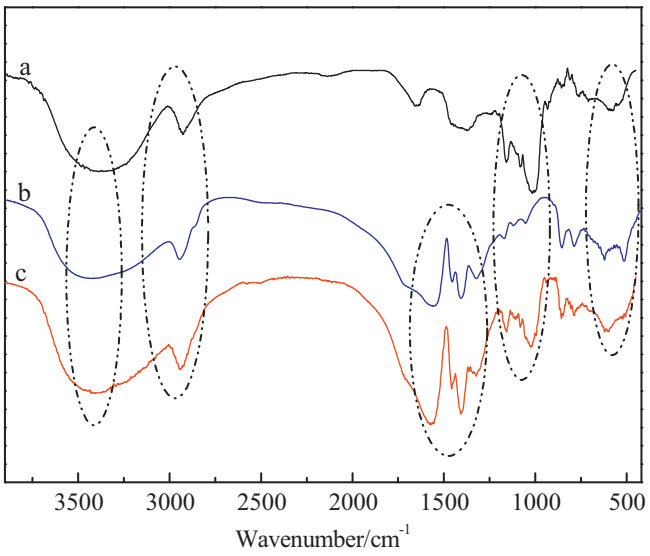

Fig. 2. FTIR spectra of (a) starch, (b) PSA and (c) St-g-SA copolymer.

CMT304 testing machine (Shenzhen, China) with a crosshead speed of 10 mm/min. Five measurements of each sample film were evaluated and the average value was taken.

3. Results and discussion

3.1. FTIR spectra analysis

The FTIR spectra of three kind model materials exhibit a similar pattern and all grafted copolymers also exhibit a similar pattern as shown in Fig. 1. The significant absorption peaks at 3385 cm^{-1} (s), 2925 cm^{-1} (m) and a triplet peak at 1156 (m), 1080 (w) and 992 cm^{-1} (s) are ascribed to the —OH stretching, C—H stretching and C—O—C stretching (Zou et al., 2012), respectively (Fig. 1a–c). The —OH and C—H stretching and bending are exhibited range from 2700 cm^{-1} to 3600 cm^{-1} (Fig. 1d–f). The absorption peaks at 1571(s) and 1409 cm^{-1} (s) indicate —COO^- (s) stretching, as shown in Fig. 1d–f (Kim, Na, Park, Yoon, & Ihm, 2002; Wu et al., 2003; Zhang et al., 2007). Furthermore, the peak at 1700–1740 cm^{-1} and 1429 cm^{-1} exhibit two very weak bands of —COOH stretching vibration, because almost all acrylic acid is neutralized by sodium hydroxide. The absorption bands at 858 cm^{-1} (w) is a peak in fingerprint region of grafted copolymers.

To demonstrate graft reaction, the FTIR spectra of starch, PSA, and grafted copolymer are illustrated in Fig. 2. Only one spectrum of starch is used to explain because three kind starches have the same FTIR spectra, so do the grafted copolymers. As can be seen, the absorption peaks in the region of 3500–3250 cm^{-1} (s) and 3000–2800 cm^{-1} (m) are related to the —OH stretching vibration and the C—H stretching vibration, respectively. Compared to starch and PSA, both group similar absorption peaks appear in 1200–900 cm^{-1} and 1600–1250 cm^{-1} (Fig. 2c). 1200–900 cm^{-1} peaks can be ascribed to the bounds C—O—C stretching vibration of starch as shown in Fig. 2a, and the peaks appearing in 1600–1250 cm^{-1} can be ascribed to the bounds —COO^- stretching vibration of sodium acrylate as shown in Fig. 2b. Besides Fig. 2c shows a particular absorption peak at 500–700 cm^{-1} which is different from starch and PSA. The peak at 500–700 cm^{-1} appearing in fingerprint region of grafted copolymer and previously mentioned two similar group absorption peaks indicate that all starches have successfully grafted onto sodium acrylate chains.

3.2. Solid state ^{13}C NMR spectral analysis

FTIR analysis gives a good indication that grafting has taken place for each of St-g-SA copolymers. However, to further confirm that grafting has taken place, solid state ^{13}C NMR spectroscopy has been carried out. Fig. 3 shows the peak assignments from the solid state ^{13}C NMR spectra of starch, copolymers and PSA. In Fig. 3a, the low filed peak at $\delta = 100.3$ ppm is due to anomeric carbon (C1), the peak at $\delta = 80.8$ ppm is due to C4. The peak in the range 71–74 ppm is for carbon atoms (C2, 3, 5) connected by —OH groups (Zhang, Xu, & Wang, 2008; Zou et al., 2012). PSA has two major peaks as shown in Fig. 3e. One peak at $\delta = 184.8$ ppm is due to carboxylic acid carbon atom. And another peak at $\delta = 45.7$ ppm can be accredited to sp^3 hybridized carbon atoms as reported previously (Sarkar, Mandre, Panda, & Pal, 2013; Zhang et al., 2008).

The solid state ^{13}C NMR spectra of copolymers show six obvious peaks (Fig. 3b–d). The carbon atom C1–C5 of glucose in starches are identified for copolymers, the peaks at $\delta = 100.3$, 80.8 and 72.1 ppm, responsible for anomeric carbon (C1), carbon atom (C4) and carbon atoms (C2, 3, 5), respectively, and there are no obvious differences

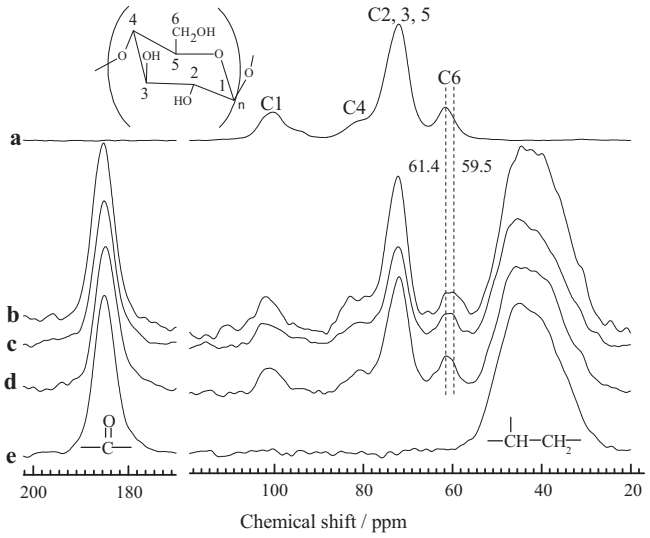

Fig. 3. Solid state ^{13}C NMR spectra of (a) starch, (b) waxy St-g-SA copolymer, (c) maize St-g-SA copolymer, (d) high amylose St-g-SA copolymer and (e) PSA.

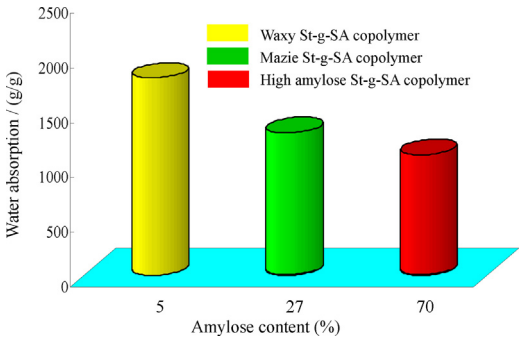

Fig. 4. Effect of amylose content on water absorbent capacity of St-g-SA copolymer.

of chemical shifts between starch and copolymers. However, a new peak is observed at $\delta = 59.5$ ppm after grafting, which appears close to the peak for C6 $\delta = 61.4$ ppm as shown in Fig. 3b and c, and a shoulder peak appears on C6 peak of starch as shown in Fig. 3d, indicating that a part of hydroxyl groups of C6 participate in graft reaction (Zhang et al., 2008; Zou et al., 2012). These results show that starch has been grafted onto sodium acrylate chains through covalent attachment further.

3.3. *Effects of amylose content on water absorbent capacity and grafting ratio*

Effects of amylose content on water absorbent capacity and grafting ratio of copolymers are shown in Fig. 4 and Table 1,

Table 1
Effect of amylose content on the grafting ratio.

Starch	Amylose content (%)	Grafting ratio (%)
Waxy	5	156.3
Maize	27	119.6
High amlyose	70	65.7

respectively. It can be clearly seen from Fig. 4 that the copolymer based on the starch with lower amylose content generally records higher water absorbency. Grafting ratio closely related to water absorption also increases with decreasing amylose content as shown in Table 1. This result is in contrast to the result reported previously by Zou et al. (2012) which studied the effects of amylose content on grafting reactions and performance of starch graft acrylamide superabsorbent polymers and the water absorbent capacity is below 1000 g/g. St-g-SA copolymers have the greater value of absorbing water due to the larger number of Na^+ inside polymeric network leading to the higher osmotic pressure than polymers which are partly saponified.

The peak of gelatinization endotherm reported appears at lower temperature for waxy starch than those of maize starch and high amylose starch and the temperature of gelatinization increases with the increase of amylose contents (Liu et al., 2006). While the decrease in elongation at break and solubility with increasing amylose content (Yun & Yoon, 2010) indicated starch with higher amylose is harder to break up double helix and is easier to flocculate after gelatinizing. These factors have a strong influence on the water absorbent capacity and grafting ratio of copolymers. In detail, the absorbency values increase remarkably with a decrease in amylose

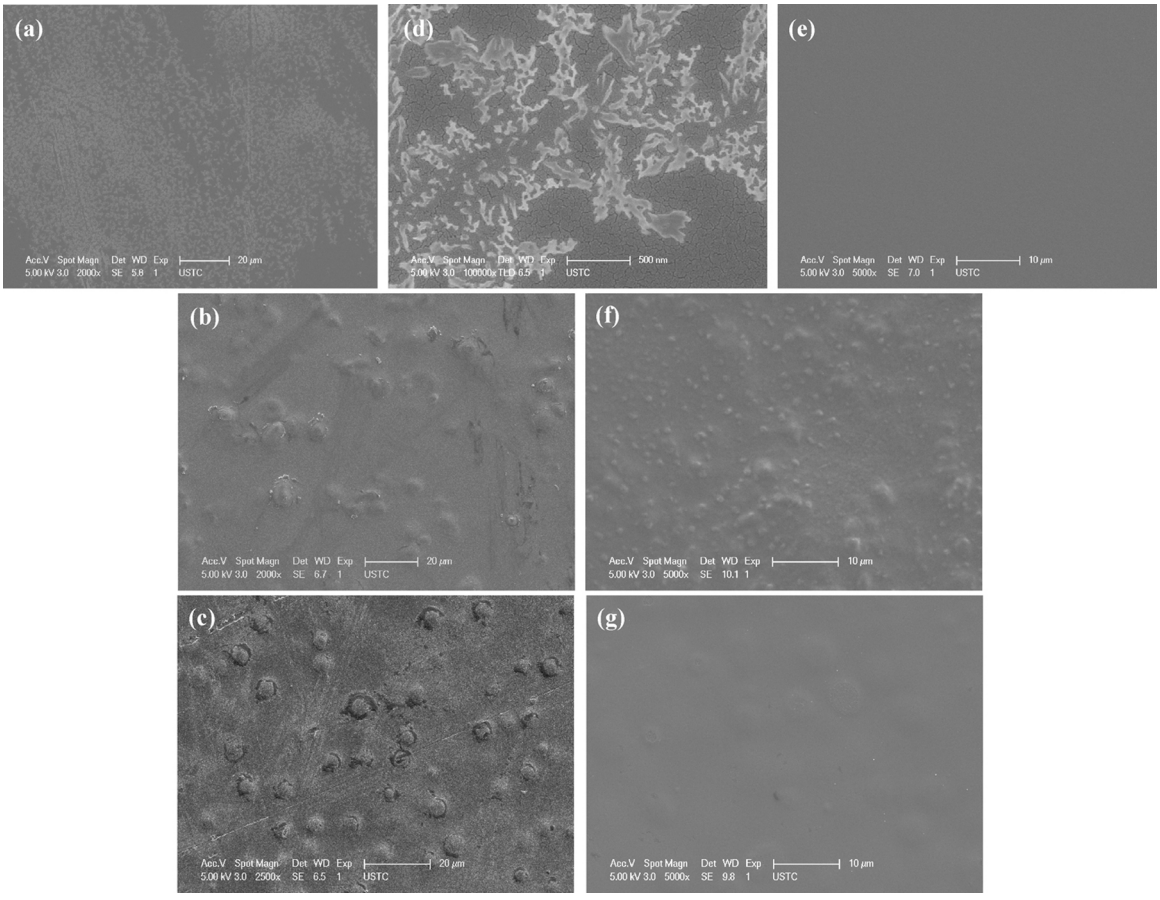

Fig. 5. SEM photographs of surfaces of (a) waxy St-g-SA copolymer, (b) maize St-g-SA copolymer, (c) high amylose St-g-SA copolymer, (d) magnification of waxy St-g-SA copolymer to 100,000×, and surfaces of (e) waxy St-g-SA copolymer, (f) maize St-g-SA copolymer and (g) high amylose St-g-SA copolymer, respectively, after being extracted with dioxane for 12 h at 105 °C.

content, partly, since incomplete gelatinized starch granules with poor absorbency decrease water absorbent capacity of copolymers. It can be inferred that lower amylose content of starch will record higher water absorbency and grafting ratio.

3.4. Morphological analysis

The morphologies of surfaces of copolymer films are illustrated Fig. 5. It can be seen from Fig. 5a that the surface of waxy St-g-SA copolymer has some arabesquitic objects like decorative patterns tending to get together to form some certain structures found by further magnifying (Fig. 5d). The surfaces of maize and high amylose St-g-SA copolymer films not only show patterns that are similar to decorative patterns on the surface of waxy St-g-SA copolymer film, but also can see some papillary protrusions. In addition, comparing Fig. 5b and c, it can be noticed that the granules on the latter are bigger than the former. The SEM photographs of surface of copolymer film being soaked into dioxane to extract arabesquitic objects with Soxhlet extraction method for 12 h at 105 °C are observed and are shown in Fig. 5e–g. Patterns on the surface of copolymers are removed resulting from dioxane dissolution. Self-polymerize of acrylic acid easily produce homopolymer. Dioxane can dissolve acrylic acid homopolymer (Witono et al., 2013), which indicates that those patterns on surfaces of copolymer are acrylic acid homopolymers. Waxy St-g-SA copolymer has a smooth surface (Fig. 5e) and maize St-g-SA copolymer has coarse surface with varied size particles, and high amylose St-g-SA copolymer has some larger particles on surface (Fig. 5g). These particles, partly dissolving or deforming owing to the change of surface tension after a long time impregnating, seem to be incomplete gelatinized starch, which can be confirmed by the following cross section SEM photographs of copolymers.

The starches and the cross sections of copolymer films are observed by scanning electron microscopy as shown in Fig. 6. The starch granules (Fig. 6a–c) have an irregular shape with smooth surface and varied particle sizes as reported previously by Lanthong et al. (2006). The cross section of waxy St-g-SA copolymer shows very smooth and homogeneous without any granules, and maize St-g-SA copolymer and high amylose St-g-SA copolymer show a coarse cross section with granules as shown in Fig. 6d–f. In addition, further magnifying also proves the same result and finds these granules are aggregation of nano particles. It can be also concluded from Figs. 5 and 6 that lack of compatibility between granules and copolymers makes a coarse surface and the nonuniform microstructure of copolymer. This observation indicates that the amylose content has obvious influence on the microstructure of copolymers.

The morphologies observed give a conjecture that those granules appearing on surface and cross section of copolymer may be incomplete gelatinized starch particles or aggregates, forming two phase system with grafted copolymer tending to separate and in-phase polymerization as shown in Fig. 6e and f. So further work was taken and the result is the proof of previous conjecture.

To demonstrate the previous conjecture, waxy, maize and high amylose starches were gelatinized at 100 °C (waxy and maize starches) and 120 °C (high amylose starch) for 30 min in an autoclave, then were poured onto a polytetrafluoroethylene dish and were dried at 65 °C for 12 h to form films, finally dried at 105 °C to a constant weight. The SEM images of starch films cross sections are shown in Fig. 7. As can be seen, the cross section of waxy starch

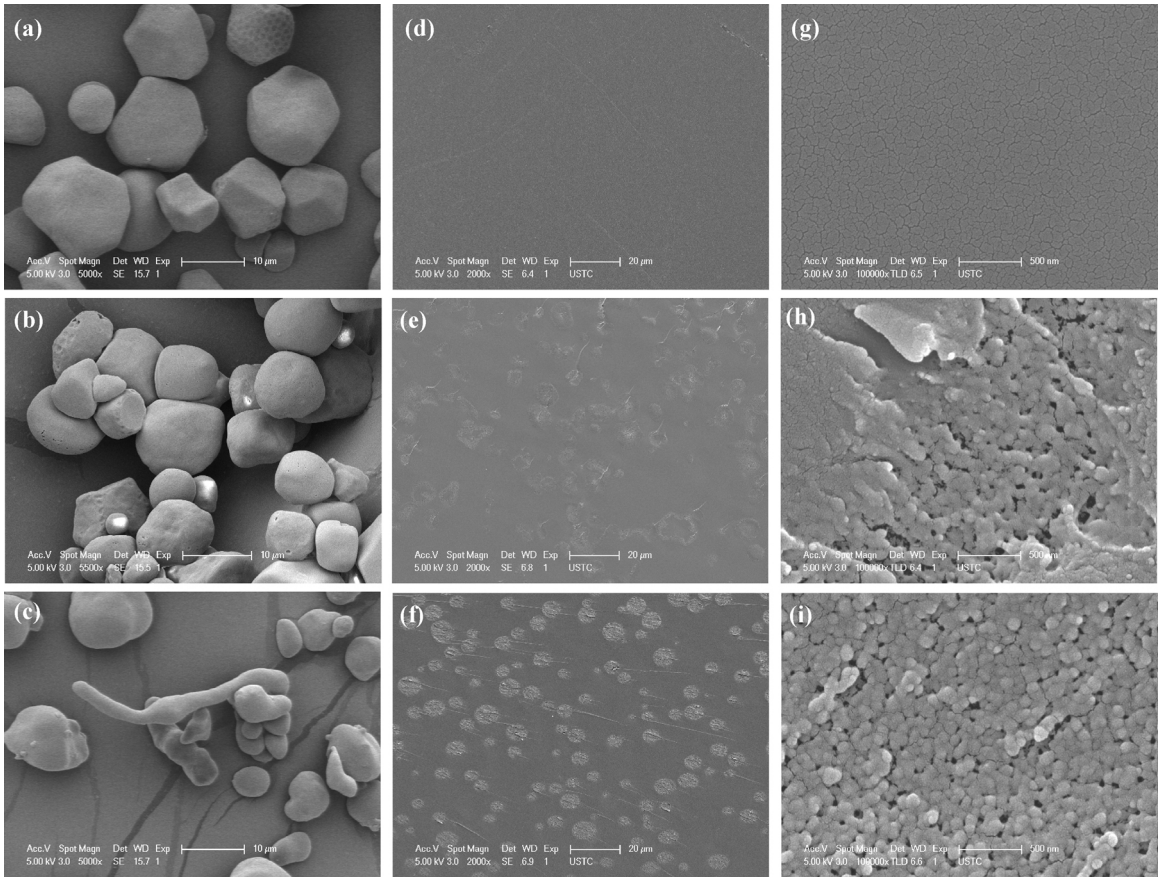

Fig. 6. SEM photographs of (a) waxy starch, (b) maize starch, (c) high amylose starch, and cross sections of (d) waxy St-g-SA copolymer, (e) maize St-g-SA copolymer, (f) high amylose St-g-SA copolymer, (g) magnification of waxy St-g-SA copolymer to 100,000×, (h) magnification of maize St-g-SA copolymer to 100,000× and (i) magnification of high amylose St-g-SA copolymer to 100,000×.

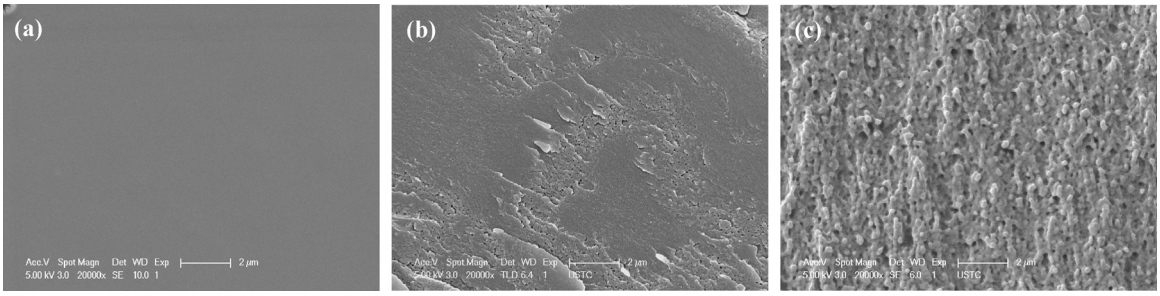

Fig. 7. SEM photographs of starch films cross sections of (a) waxy starch, (b) maize starch and (c) high amylose starch.

film is smooth and homogeneous while the maize starch film is relatively coarse with small particles. Fig. 7c shows that the film of high amylose starch almost completely become nano particles, which indicates that those nano granules are incomplete gelatinized starch aggregates (Koch, Gillgren, Stading, & Andersson, 2010), corresponding to the phenomenons appearing Fig. 5c and Fig. 6f. According to the above observations from SEM, it can be concluded that the degree of starch gelatinization increases with a decrease in amylose content and water absorbent capacity is also affected with amylose content via affecting the microstructure of copolymers. The microstructure of waxy St-g-SA copolymer is smooth and homogeneous so that water can fully permeate into the polymeric network until equilibrium reaches and the network holds a considerable volume of liquids by osmotic pressure between Na^+ solution inside copolymer network and free water out of copolymer network. However, incomplete gelatinized starch aggregates exist in maize St-g-SA copolymer but not in resin chains, which will reduce ingress of water and water absorption capacity. Certainly, high amylose St-g-SA copolymer having more particles leads to lower water absorption than the former.

The above results of SEM photographs are consistent with water absorbent capacity and grafting ratio. In a word, waxy St-g-SA copolymer has smooth, homogeneous microstructure, high water absorbent capacity and high grafting ratio since waxy starch containing low amylose content is favorable for gelatinization and grafting.

3.5. *Dynamic mechanical thermal analysis (DMTA) and mechanical properties*

The thermograms of PSA and copolymers are shown in Fig. 8. It can be seen that there are two thermal transitions in each thermogram. The first peak at a low temperature range can be attributed to some water induced relaxtion due to polymers strong hydrophilicity. Moreover, this peak shifts to higher temperature with the increase of amylose content, corresponding to the water absorbent capacity of polymers. And the second higher and obvious thermal transitions rang between 145 and 175 °C. The DMTA results demonstrate that the values of transition peak of copolymers are higher than that of PSA, which indicates that grafting will increase the value of transition peak by increasing the thermal energy required to free polymer molecules from additional constraints (Kennedy, Lyons, Geever, & Higginbotham, 2009).

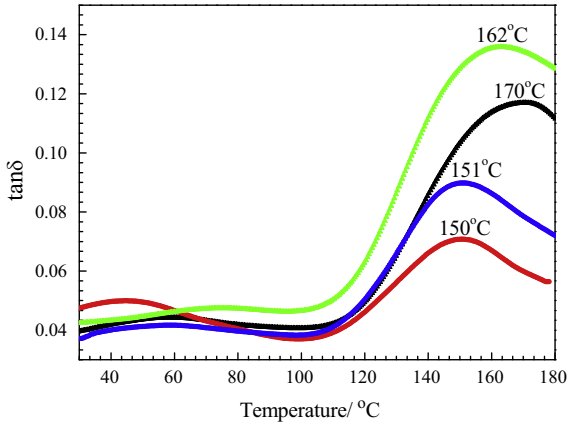

Fig. 8. DMTA curves (tan δ) as a function of temperature for polymers.

In Fig. 8, the second transtion temperature of waxy St-g-SA copolymer is the highest due to the reduction in the mobility of kinetic units as a result of grafting and crosslinking (Kennedy et al., 2009), which implies that waxy St-g-SA copolymer has higher grafting ratio. The value of high amylose St-g-SA copolymer is relative high. This is attributed to two reasons: one is that amylose is a linear molecule with an extended helical twist (Yun & Yoon, 2010) and its move depends on long segments or even the whole chain. Another is that most remnant rigid starch granules (shown in Fig. 6f) embed in entangled matrix content amylose and amylopectin network in copolymer, which might deteriorate the mobility and orientation of molecular chain by physical cross-links (Wang, Yu, Chang, & Ma, 2008). The value of maize St-g-SA copolymer is close to PSA, which is mainly related to few remnant starch granules (shown in Fig. 6e). To some extent, these thermograms reflect the microphase separation which exists within starches and grafted copolymers, corresponding to the results of SEM.

The elongation at break of PSA, waxy, maize and high amylose St-g-SA polymer is 117%, 239%, 152% and 187%, respectively. The elongations at break of copolymers are higher than that of PSA. The elongation at break of waxy St-g-SA copolymer is the highest, which attributes to its high grafting ratio. However, the high amylose St-g-SA copolymer has rather high elongation at break, it could be explained that the copolymer was enhanced by the ungrafted high amylose starch (Yun & Yoon, 2010). The results are related to that of DMTA.

4. Conclusions

In this study, the property and microstructure of St-g-SA copolymers based on three kind starches with different amylose content have been investigated.

The FTIR and solid state ^{13}C NMR results indicated that three kind starches were successfully grafted onto sodium acrylate chains. The water absorbent capacity of waxy, maize and high amylose St-g-SA copolymers is 1800 g/g, 1300 g/g and 1100 g/g, respectively. Grafting ratio also increased with decreasing amylose content. SEM results indicated that waxy St-g-SA copolymer film was smooth and homogeneous, and microstructures of maize and high amylose St-g-SA copolymers were heterogeneous showing incomplete gelatinized starch aggregates on surface and cross section. St-g-SA copolymers based on lower amylose content had smoother surface, cross section and more homogeneous

microstructure and better properties of grafting ratio and water absorption than those based on higher amylose content. The DMTA results shown graft copolymerization increased the value of transition temperature, the waxy St-g-SA copolymer had the highest transition temperature which indicated waxy starch had high grafting ratio.

Acknowledgments

The authors would like to thank the National Natural Science Foundation of China (grant no. 31171655) and Natural Science Foundation of Anhui Provincial Education Department (KJ2012Z104) for financial support.

References

Ameye, D., Voorspoels, J., Foreman, P., Tsai, J., Richardson, P., Geresh, S., et al. (2001). Trypsin inhibition, calcium and zinc ion binding of starch-g-poly(acrylic acid) copolymers and starch/poly(acrylic acid) mixtures for peroral peptide drug delivery. *Journal of Controlled Release*, *75*, 357–364.

Ameye, D., Voorspoels, J., Foreman, P., Tsai, J., Richardson, P., Geresh, S., et al. (2002). Ex vivo bioadhesion and in vivo testosterone bioavailability study of different bioadhesive formulations based on starch-g-poly(acrylic acid) copolymers and starch/poly (acrylic acid) mixtures. *Journal of Controlled Release*, *79*, 173–182.

Athawale, V. D., & Lele, V. (2001). Recent trends in hydrogels based on starch-graft-acrylic acid: A review. *Starch/Stärke*, *53*, 7–13.

Cao, L. Q., Xu, S. M., Feng, S., & Wang, J. D. (2005). Swelling and thermal behaviors of a starch-based superabsorbent hydrogel with quaternary ammonium and carboxyl groups. *Journal of Applied Polymer Science*, *96*, 2392–2398.

Coucke, D., Schotsaert, M., Libert, C., Pringels, E., Vervaet, C., Foreman, P., et al. (2009). Spray-dried powders of starch and crosslinked poly(acrylic acid) as carriers for nasal delivery of inactivated influenza vaccine. *Vaccine*, *27*, 1279–1286.

Eid, M. (2008). In vitro release studies of vitamin B_{12} from poly N-vinyl pyrrolidone/starch hydrogels grafted with acrylic acid synthesized by gamma radiation. *Nuclear Instruments and Methods in Physics Research B: Beam Interactions with Materials and Atoms*, *266*, 5020–5026.

Güçlü, G., Güçlü, K., & Keleş, S. (2007). Competitive removal of nickel (II), cobalt (II), and zinc (II) ions from aqueous solutions by starch-graft-acrylic acid copolymers. *Journal of Applied Polymer Science*, *106*, 1800–1805.

Güçlü, G., Al, E., Emik, S., İyim, T. B., Özgümüş, S., & Özyürek, M. (2010). Removal of Cu^{2+} and Pb^{2+} ions from aqueous solutions by starch-graft-acrylic acid/montmorillonite superabsorbent nanocomposite hydrogels. *Polymer Bulletin*, *65*, 333–346.

Hua, S. B., & Wang, A. Q. (2008). Preparation and properties of superabsorbent containing starch and sodium humate. *Polymers for Advanced Technologies*, *19*, 1009–1014.

Jiraprasertkul, W., Nuisin, R., Jinsart, W., & Kiatkamjornwong, S. (2006). Synthesis and characterization of cassava starch graft poly(acrylic acid) and poly[(acrylic acid)-co-Acrylamide] and polymer flocculants for wastewater treatment. *Journal of Applied Polymer Science*, *102*, 2915–2928.

Jyothi, A. N., & Carvalho, A. J. F. (2013). Starch-g-Copolymers: Synthesis, properties and applications. In S. Kalia, & M. W. Sabaa (Eds.), *Polysaccharide based graft copolymers* (pp. 59–109). Berlin: Springer Berlin Heidelberg.

Kennedy, J. E., Lyons, J. G., Geever, L. M., & Higginbotham, C. L. (2009). Synthesis and characterisation of styrene butadiene styrene-g-acrylic acid for potential use in biomedical applications. *Materials Science & Engineering C-Biomimetic and Supramolecular Systems*, *29*, 1655–1661.

Kim, D. H., Na, S. K., Park, J. S., Yoon, K. J., & Ihm, D. W. (2002). Studies on the preparation of hydrolyzed starch-g-PAN (HSPAN)/PVA blend films—Effect of the reaction with epichlorohydrin. *European Polymer Journal*, *38*, 1199–1204.

Kiseleva, V. I., Krivandin, A. V., Fornal, J., Błaszczak, W., Jeliński, T., & Yuryev, V. P. (2005). Annealing of normal and mutant wheat starches. LM, SEM, DSC, and SAXS studies. *Carbohydrate Research*, *340*, 75–83.

Koch, K., Gillgren, T., Stading, M., & Andersson, R. (2010). Mechanical and structural properties of solution-cast high-amylose maize starch films. *International Journal of Biological Macromolecules*, *46*, 13–19.

Lanthong, P., Nuisin, R., & Kiatkamjornwong, S. (2006). Graft copolymerization, characterization, and degradation of cassava starch-g-acrylamide/itaconic acid superabsorbents. *Carbohydrate Polymers*, *66*, 229–245.

Liu, H. S., Yu, L., Xie, F. W., & Chen, L. (2006). Gelatinization of cornstarch with different amylose/amylopectin content. *Carbohydrate Polymers*, *65*, 357–363.

Matveev, Y. I., Van Soest, J. J. G., Nieman, C., Wasserman, L. A., Protserov, V. A., Ezernitskaja, M., et al. (2001). The relationship between thermodynamic and structural properties of low and high amylose maize starches. *Carbohydrate Polymers*, *44*, 151–160.

Sang, Y. J., Bean, S., Seib, P. A., Pedersen, J., & Shi, Y. C. (2008). Structure and functional properties of sorghum starches differing in amylose content. *Journal of Agricultural and Food Chemistry*, *56*, 6680–6685.

Sarkar, A. K., Mandre, N. R., Panda, A. B., & Pal, S. (2013). Amylopectin grafted with poly (acrylic acid): Development and application of a high performance flocculant. *Carbohydrate Polymers*, *95*, 753–759.

Wang, N., Yu, J. G., Chang, P. R., & Ma, X. F. (2008). Influence of formamide and water on the properties of thermoplastic starch/poly(lactic acid) blends. *Carbohydrate Polymers*, *71*, 109–118.

Witono, J. R., Marsman, J. H., Noordergraaf, I.-W., Heeres, H. J., & Janssen, L. P. B. M. (2013). Improved homopolymer separation to enable the application of 1 H NMR and HPLC for the determination of the reaction parameters of the graft copolymerization of acrylic acid onto starch. *Carbohydrate Research*, *370*, 38–45.

Wu, C. S. (2005). Improving polylactide/starch biocomposites by grafting polylactide with acrylic acid-characterization and biodegra-dability assessment. *Macromolecular Bioscience*, *5*, 352–361.

Wu, J. H., Wei, Y. L., Lin, J. M., & Lin, S. B. (2003). Study on starch-graft-acrylamide/mineral powder superabsorbent composite. *Polymer*, *44*, 6513–6520.

Yun, Y. H., & Yoon, S. D. (2010). Effect of amylose contents of starches on physical properties and biodegradability of starch/PVA-blended films. *Polymer Bulletin*, *64*, 553–568.

Zhang, J. P., Wang, Q., & Wang, A. Q. (2007). Synthesis and characterization of chitosan-g-poly(acrylic acid)/attapulgite superabsorbent composites. *Carbohydrate Polymers*, *68*, 367–374.

Zhang, Q., Xu, K., & Wang, P. (2008). Study on structure and molecular dynamics of starch/poly(sodium acrylate)-grafted superabsorbent by ^{13}C solid state NMR. *Fibers and Polymers*, *9*, 271–275.

Zhu, Z., Li, M., & Jin, E. (2009). Effect of an allyl pretreatment of starch on the grafting efficiency and properties of allyl starch-g-poly(acrylic acid). *Journal of Applied Polymer Science*, *112*(5), 2822–2829.

Zou, W., Yu, L., Liu, X. X., Chen, L., Zhang, X. Q., Qiao, D. L., et al. (2012). Effects of amylose/amylopectin ratio on starch-based superabsorbent polymers. *Carbohydrate Polymers*, *87*, 1583–1588.